



Published in final edited form as:

*J Mol Cell Cardiol.* 2020 January ; 138: 12–22. doi:10.1016/j.yjmcc.2019.09.015.

## Conversion of Human Cardiac Progenitor Cells into Cardiac Pacemaker-like Cells

Suchi Raghunathan<sup>1</sup>, Jose Francisco Islas<sup>2</sup>, Brandon Mistretta<sup>3</sup>, Dinakar Iyer<sup>3</sup>, Liheng Shi<sup>4</sup>, Preethi H. Gunaratne<sup>3</sup>, Gladys Ko<sup>4</sup>, Robert J. Schwartz<sup>3,\*</sup>, Bradley K. McConnell<sup>1,†,\*</sup>

<sup>1</sup>Department of Pharmacological and Pharmaceutical Sciences, College of Pharmacy, University of Houston, Houston, TX 77204-5037, USA.

<sup>2</sup>Department of Biochemistry and Molecular Medicine, Autonomous University of Nuevo León, Monterrey, Mexico.

<sup>3</sup>Department of Biology and Biochemistry, University of Houston, Houston, TX 77204-5001, USA.

<sup>4</sup>Department of Veterinary Integrative Biosciences, Texas A&M University, College Station, TX 77843-4458, USA.

### Abstract

We used a screening strategy to test for reprogramming factors for the conversion of human cardiac progenitor cells (CPCs) into Pacemaker-like cells. Human transcription factors *SHOX2*, *TBX3*, *TBX5*, *TBX18*, and the channel protein *HCN2*, were transiently induced as single factors and in trio combinations into CPCs, first transduced with the connexin 30.2 (CX30.2) mCherry reporter. Following screens for reporter CX30.2 mCherry gene activation and FACS enrichment, we observed the definitive expression of many pacemaker specific genes; including, *CX30.2*, *KCNN4*, *HCN4*, *HCN3*, *HCN1*, and *SCN3b*. These findings suggest that the *SHOX2*, *HCN2*, and *TBX5* (SHT5) combination of transcription factors is a much better candidate in driving the CPCs into Pacemaker-like cells than other combinations and single transcription factors. Additionally, single-cell RNA sequencing of SHT5 mCherry<sup>+</sup> cells revealed cellular enrichment of pacemaker

\***ADDRESS FOR CORRESPONDANCE:** Bradley K. McConnell, PhD, FAHA, FCVS, Associate Professor of Pharmacology, Department of Pharmacological and Pharmaceutical Sciences, University of Houston College of Pharmacy, 4849 Calhoun Road, Health-2 (H2) Building, Room 5024, Houston, TX 77204-5037; Phone: 713-743-1218; Fax: 713-743-1232, bkmconn@central.uh.edu.

†co-senior authors

#### AUTHORSHIP CONTRIBUTIONS:

S.R., R.J.S., and B.K.M. conceived and designed the research;

S.R., J.F.I., B.M., D.I., and L.S. conducted experiments;

S.R., R.J.S., and B.K.M. contributed new reagents or analytic tools;

S.R., J.F.I., B.M., D.I., L.S., P.G., G.K., R.J.S., and B.K.M. performed data analysis and interpreted the results;

S.R., J.F.I., B.M., D.I., L.S., G.K., R.J.S., and B.K.M. wrote or contributed to the writing of the manuscript.

#### DISCLOSURES:

Authors declare no conflicts of interests.

#### DATA AND MATERIALS AVAILABILITY STATEMENT:

The data will be made available according to the policies of *Science Translational Medicine* and of the *National Academy of Sciences (NAS)* for the open sharing of publication-rated data.

**Publisher's Disclaimer:** This is a PDF file of an unedited manuscript that has been accepted for publication. As a service to our customers we are providing this early version of the manuscript. The manuscript will undergo copyediting, typesetting, and review of the resulting proof before it is published in its final form. Please note that during the production process errors may be discovered which could affect the content, and all legal disclaimers that apply to the journal pertain.

specific genes including *TBX3*, *KCNN4*, *CX30.2*, and *BMP2*, as well as pacemaker specific potassium and calcium channels (*KCND2*, *KCNK2*, and *CACNB1*). In addition, similar to human and mouse sinoatrial node (SAN) studies, we also observed the down-regulation of *NKX2.5*. Patch-clamp recordings of the converted Pacemaker-like cells exhibited *HCN* currents demonstrated the functional characteristic of pacemaker cells. These studies will facilitate the development of an optimal Pacemaker-like cell-based therapy within failing hearts through the recovery of SAN dysfunction.

## ONE SENTENCE SUMMARY

The *SHOX2*, *HCN2*, and *TBX5* (SHT5) combination of transcription factors and channel proteins can be used to reprogram CPCs into Pacemaker-like cells as a potential stem cell therapy for sick sinus syndrome (SSS).

## Keywords

hADMSCs; CPCs; sinoatrial node; *HCN*; pacemaker cells

## INTRODUCTION

The electrical cardiac conduction system (CCS), which includes the sinoatrial node (SAN), atrioventricular node (AVN) and the Purkinje fibers, coordinates the heart's rate and rhythm (1). The SAN is responsible for initiating electric impulses down through a hierarchical pattern of the CCS to coordinate the asynchronous contractions of the atria and ventricles (2). However, failure of the SAN or a block at any point in the CCS results in arrhythmias. One major conduction disorder that results in cardiac arrhythmias is sick sinus syndrome (SSS); in which the SAN does not function properly (3). Failure of the SAN has been attributed to multiple factors including congenital defects, sarcoidosis (infections), and cardiomyopathies. Further, myocardial ischemia (MI) results in cardiomyocyte loss and scar formation, thereby creating a mechanical barrier and abnormal electrical conduction; eventually contributing to the development of cardiac arrhythmias. Furthermore, heart rhythm abnormalities are often caused or worsened by medications and these abnormalities increase with age (4). In order to circumvent these problems, the focus over the past decade has been on the development of biological pacemakers, as an alternative treatment for conduction system disorders, cardiac repair after an MI, and the limitations of the electronic pacemaker.

The SAN is the primary pacemaker of the heart and is responsible for generating the electric impulse or beat (5). Native cardiac pacemaker cells are anatomically confined within the SAN, a small structure comprised of just a few thousand specialized pacemaker cells (6). During embryonic development, the cardiac pacemaker cells originate from a subset of progenitors distinct from the first cells marked by *NKX2.5* (7) and reviewed in Burkhard et al (8). *SHOX2*, a member of the short stature paired-homeodomain family of transcription factors, is a major genetic determinant of the SAN genetic pathway and is restrictedly expressed in the region of the SAN (9). *SHOX2* inhibits *NKX2.5* expression and activates a pacemaker genetic pathway that results in up-regulation of the *GATA6* and *TBX3*

transcription factors, and *HCN4* channel (10). Along with the T-box transcription factor *TBX3*, *TBX2* maintains *SHOX2* marked cells in a state characteristic that of pacemaker-nodal cardiac myocytes (11). Other T-box transcription factors, such as *TBX5* and *TBX18*, may also stimulate pacemaker cell activity through unknown mechanisms (12, 13).

Cell-based cardiac tissue engineering strategies may, therefore, provide regenerative therapeutic options of equivalent function to mechanical and electrical devices. To reinforce this notion, we have reprogrammed human adipogenic mesenchymal stem cells (hADMSCs) into cardiac progenitor cells (CPCs) with ETS2 and MESP1, as co-activators of cardiac differentiation (14). Human ADMSCs are ideal for cell-based therapies since they can be obtained from self-donor patients, treated, and transplanted back to the patient without the burden of immune rejection and or tumor formation (15). Clinical trials worldwide involving hADMSCs in the treatment of human disease ([clinicaltrials.gov](http://clinicaltrials.gov)) have been proven safe and preserved ventricular function in patients (15); however, hADMSCs have failed to be successfully reprogrammed into either cardiac myocytes, vascular cells, pacemaker cell, or Purkinje cells. Although several recent studies have indicated the potential of hADMSCs for cardiac conversion (15–17), no study has convincingly demonstrated their conversions to conduction cells such as pacemaker cells and/or Purkinje cells. Our strategy was to use reprogrammed human CPCs (14) in a novel screening assay using a variety of transcription factors and channel proteins to convert into human cardiac Pacemaker-like cells.

## MATERIAL AND METHODS

### Reprogramming of hADMSCs into CPCs

Human ADMSCs (hADMSCs) were reprogrammed into CPCs using the human transcription factors ETS2/MESP1 for the differentiation of human cardiac fibroblasts into CPCs (14). Initially, hADMSCs were pre-infected with NKX2.5 td-tomato puromycin reporter, followed by treatment with TAT-fused proteins ETS2 and MESP1 for 3-days, at a concentration of 50  $\mu$ M each. Subsequently, these cells were forced aggregated (600 cells per aggregate) and kept in hanging drops for 2-days. Afterward, the cells were plated and treated with Activin and BMP (2-days) with normal media change. On activation of NKX2.5 td-tomato reporter, the marker for CPC development, the cells were drug selected via puromycin (2-days drug selection and left for an additional 8-days to grow).

### Conversion of CPCs into Pacemaker-like Cells

Reprogramming of CPCs was initially accomplished by infecting 70–80% confluent plates with rtTA2 lentiviral vector and pWPI-CX30.2-puro IRES mCherry reporter lentiviral pacemaker-specific vectors for tracking and flow cytometry sorting of reprogrammed cells. To reprogram CPCs into Pacemaker-like cells, *CX30.2* vector infected CPCs were split into eight plates and infected with pDox-*SHOX2*-eGFP, pDox-*HCN2*-eGFP, pDox-*TBX3*-eGFP, pDox-*TBX5*-eGFP, and pDox-*TBX18*-eGFP individually and in multiple combinations for transient gene expression. Lentiviral infected cultures were treated with 1  $\mu$ g/ml doxycycline for 3-days to induce transient transcription factor expression. After 3-days, the doxycycline-induced expressed enhanced Green Fluorescent Protein (eGFP) labeled transcription factors were then observed under the microscope and the expressed transcription factor proteins

were confirmed by Western blot of cell lysates. On day-4, all the different combinations were FACS sorted for eGFP+ cells and cultured under similar conditions as CPCs. After a week, the eGFP+ cells were FACS sorted for mCherry+ cells, followed by gene expression analysis by RT-PCR, patch-clamp recording, RNA sequencing, and single-cell RNA sequencing studies.

### Cell Culture

CPCs were cultured in alpha-MEM (Life Technologies Corporation) supplemented with 1% (v/v) 1X Glutamax (Life Technologies Corporation), 10% (v/v) FBS (GenDEPOT) and 100 U/ml penicillin. Media for cells was changed every 2-days. Cells were washed twice with Dulbecco's phosphate-buffered saline (GenDEPOT) prior to trypsin-EDTA (1X) (GenDEPOT) treatment with the purpose of passaging, FACS sorting, other downstream experiments, and freezing. Cell freezing media was composed of alpha-MEM supplemented with 20% (v/v) FBS and 7–8% (v/v) DMSO. Transient gene expression was induced by supplementing the cell culture media with doxycycline (1µg/ml) (Clontech). 293T cells were cultured in DMEM (Life Technologies Corporation) supplemented with 10% (v/v) FBS and 100U/ml penicillin. Control CPCs were cultured for the same amount of time as the lentiviral infected CPC cultures.

### Plasmid Extraction

All the plasmid DNA which was used for transfection were amplified by transforming into DH5 alpha cells. Plasmid DNA was extracted using a maxi prep kit according to the manufacturer's instructions (#12162, Qiagen) and quantified using Nanodrop.

### Lentiviral Production and Transduction

Lentivirus production for all the plasmids was carried out in 70–80% confluent HEK-293T cells (DNA : transfection reagent; 1:2) using JetPrime transfection reagent (Polyplus-transfection) according to the manufacturer's instruction. Viral supernatant collected at 48 and 72 hours was filtered through 0.45 µm cellulose filter and then concentrated using Lenti-X concentrator (#631232, Takara Bio USA, Inc.) following the manufacturer's protocol. For virus transduction, the virus was added to alpha-MEM media containing polybrene at 8 µg/ml concentration. Twenty-four hours after plating the CPCs, the alpha-MEM media was replaced with viral media containing freshly made polybrene. After 24 h, the viral media was replaced with fresh media.

### Western Blot Analysis

The cell samples were lysed using radioimmunoprecipitation assay (RIPA) buffer supplemented with protease inhibitor cocktail (P8340, Sigma Aldrich). Lysed samples were denatured by boiling at 100°C for 5 minutes with NuPAGE LDS Sample Buffer (NP0007, Life Technologies) and subjected to electrophoresis with Novex NUPAGE system. This was followed by transferring protein onto polyvinylidene difluoride (PVDF) membranes. The membranes were blocked with 5% milk for an hour. The blots were then treated with primary antibodies overnight, followed by TBS (0.1% tween 20) wash 3 times each for 5 minutes. Then the membranes were probed with horseradish peroxidase (HRP) conjugated

secondary antibody for 2 hours at RT. The blots were developed using Enhanced Chemiluminescence Western Lightning Plus (Cat #NEL104001EA, Perkin Elmer).

| Primer             | Sequence          | Concentration | Primerbank ID            |
|--------------------|-------------------|---------------|--------------------------|
| <b>SHOX2</b>       | Mouse Monoclonal  | 1:1000        | Sigma Aldrich            |
| <b>HCN2</b>        | Rabbit Monoclonal | 1:1000        | Celi Signaling           |
| <b>TBX3</b>        | Mouse Monoclonal  | 1:1000        | Santa Cruz Biotechnology |
| <b>HA-Tag</b>      | Mouse Monoclonal  | 1:1000        | GenDEPOT                 |
| <b>TBX18</b>       | Mouse Monoclonal  | 1:1000        | Santa Cruz Biotechnology |
| <b>Anti-mouse</b>  |                   | 1:10,000      | Celi Signaling           |
| <b>Anti-rabbit</b> |                   | 1:10,000      | Celi Signaling           |

List of antibodies, species, their concentration, and company.

### Fluorescence Microscopy

Brightfield and fluorescence images of cell cultures were acquired using a Nikon Ti-E inverted microscope attached with a DS-Fi 1 5-megapixel color camera (Nikon Instruments). Images were captured and analyzed using NIS Elements software v4.13 (Nikon Instruments).

### FACS Analysis and Sorting

CPCs at the time-points mentioned were first washed with PBS twice and then dissociated using 0.25% trypsin. Following which the cells were then neutralized using FBS and centrifuged at 1000 rpm for 5 min to get the cell pellet. The cell pellet was then resuspended in alpha-MEM supplemented with 1% FBS, counted using hemocytometer and diluted to obtain  $1-1.5 \times 10^6$  cells/ml. The cells were then passed through a cell strainer and into a conical FACS tube. A BD LSRII flow cytometer (BD Biosciences) was used to perform FACS analysis and then subsequently followed by sorting on a FACSaria II flow cytometer (BD Biosciences). Sorted cells were collected in alpha-MEM supplemented with 50% FBS and then plated on cell culture plates.

### RNA Isolation and Real-time RT-PCR analysis

RNA was isolated from mCherry+ cells after FACS sorting by following the manufacturer's instructions (R1054, Zymo Research) and quantified using Nanodrop. cDNA synthesis was performed using a high capacity RT-PCR kit (#4368814, Life Technologies) according to the manufacturer's instructions. cDNA was subjected to qRT-PCR using Power SYBR Green PCR Master Mix (#4367659, Life Technologies) in a StepOnePlus Real-Time PCR System (v. 2.0, Applied Biosystems). Normally, all the real-time PCR reactions were carried out as 15  $\mu$ L reactions in 96-well plates. Each reaction mixture contained 1  $\mu$ L diluted cDNA, 2  $\mu$ L each of forward and reverse primers (10  $\mu$ M), 7.5  $\mu$ L 2X SYBR Green PCR Master Mix, and 2.5  $\mu$ L water. PCR primers were from the PrimerBank database (18). Normalization was performed using GAPDH mRNA levels.

| Primer                         | Sequence                      | Primerbank ID |
|--------------------------------|-------------------------------|---------------|
| <b>HCN1 – forward</b>          | 5' CATGCCACCGCTTAAATCCAG 3'   | 349501105c2   |
| <b>HCN1 – reverse</b>          | 5' ATTGTAGCCACCAGTTTCCGA 3'   |               |
| <b>HCN3 – forward</b>          | 5' AGCAGTGGAAATCGAGCAGG 3'    | 38327036c2    |
| <b>HCN3 – reverse</b>          | 5' GGTCACAGTAAAACCGGAAGT 3'   |               |
| <b>HCN4 – forward</b>          | 5' GAACAGGAGAGGGTCAAGTCG 3'   | 210147528c2   |
| <b>HCN4 – reverse</b>          | 5' CATTGAAGACAATCCAGGGTGT 3'  |               |
| <b>SCN3b – forward</b>         | 5' GCCTTCAATAGATTGTTCCCT 3'   | 93587331c1    |
| <b>SCN3b – reverse</b>         | 5' CTCGGGCCTGTAGAACCAT 3'     |               |
| <b>Cx30.2 (GJC3) – forward</b> | 5' TGGAGTCAGCGTTTCTGTC 3'     | 289177042c3   |
| <b>Cx30.2 (GJC3) – reverse</b> | 5' TTGTGCTTCTGGTGCTCTCT 3'    |               |
| <b>KCNN4 – forward</b>         | 5' CTGCTGCGTCTCTACCTGG 3'     | 25777651c1    |
| <b>KCNN4 – reverse</b>         | 5' AGGGTGCGTGTTCATGTAAAG 3'   |               |
| <b>GAPDH – forward</b>         | 5' GGAGCGAGATCCCTCCAAAAT 3'   | 378404907c1   |
| <b>GAPDH – reverse</b>         | 5' GGCTGTTGTCATACTTCTCATGG 3' |               |

Primer sequences with their respective Primerbank ID.

### Patch Clamp Electrophysiology

Whole-cell voltage-clamp recordings were carried out on each cell line [CPCs (control) and SHT5 mCherry+ FACS sorted cells (reprogrammed)]. The external solution for *HCN* currents contained the following (in mM): 140 NaCl, 5.4 KCl, 1 MgCl<sub>2</sub>, 5 BaCl<sub>2</sub>, 2 CoCl<sub>2</sub>, 0.5 4-aminopyridine, 10 glucose, 5 HEPES, 1.8 CaCl<sub>2</sub> and with the pH adjusted to 7.4 with NaOH. Cesium chloride (CsCl, 5 mM) was added to the external solution as the Cs<sup>+</sup> external solution. The pipette solution was (in mM): 130K-aspartate, 5 Na<sub>2</sub>-ATP, 5 CaCl<sub>2</sub>, 2 MgCl<sub>2</sub>, 11 EGTA, 10 HEPES and with the pH adjusted to 7.35 with KOH. A patch-clamp amplifier (Model 2400. A-M Systems, Carlsborg, WA, USA) was used to record currents at room temperature. This was followed by low pass-filtering of signals at 2 kHz and using the Digidata 1550A interface and pCLAMP 10.5 software (Axon Instruments/Molecular Devices, Union City, CA, USA) for digitizing signals at 5 kHz. Electrode capacitance was compensated after the formation of gigaohm signals.

A 5 mV (100 ms) depolarizing voltage step was applied from –40 mV of holding potential to record series and input resistance as well as membrane capacitance for the recorded cells. Whole-cell capacitance value was determined from the membrane capacitance reading (19). Cells were held at –40 mV, and the *HCN* currents were recorded immediately after the whole-cell configurations were formed using beta-escin (50 μM, Sigma). The current was elicited from a holding potential at –40 mV and a hyperpolarizing step to –130mV for 1.5 sec. Each cell was first recorded with the regular external solution (without Cs<sup>+</sup>) followed by recording with the Cs<sup>+</sup>-external solution. In order to completely exchange the buffer, the recording chamber was perfused with Cs<sup>+</sup> external buffer for at least 2 min. The current density (pA/pF) was obtained by dividing the current amplitude (pA) with the membrane capacitance (pF).

A series of hyperpolarizing step command (from –135 mV to –55 mV with a 10 mV increment, each step for 3 sec) followed by a depolarization step (to +5 mV for 1 sec) was applied to determine the channel activation kinetics. To generate the activation curve, the Cs



+ sensitive current at each voltage-step (I) was normalized to the peak current (I<sub>max</sub> at -135 mV), and the I/I<sub>max</sub> was plotted then fitted with the Boltzmann equation:  $I/I_{max} = 1 / [1 + \exp((V_{1/2} - V) / k)]$ . The voltage that elicited half of the maximal current was also determined as V<sub>1/2</sub>. For isoproterenol (ISO) treatment, the 0.5 mM ISO in DMSO stock solution was prepared freshly and diluted with the culture medium. The cells were incubated for 1 h in the presence of 100 nM ISO or the vesicle DMSO (as the control). Then the cells subjected to patch-clamp recordings. All data are presented as mean ± standard error of mean (s.e.m.). The Student's t-test was used for the statistical analyses. Throughout, \*p<0.05 was regarded as significant.

### RNA-Sequencing Library Preparation and Sequencing

RNA was extracted using Mirneasy Mini Kit (Qiagen) with on-column RNase-Free DNase (Qiagen) digestion following the manufacturer's instructions. Extracted RNA samples underwent quality control assessment using the RNA Nano 6000 chip on Bioanalyzer 2100 (Agilent) and were quantified with Qubit Fluorometer (Thermo Fisher). The RNA libraries were prepared and sequenced at the University of Houston Seq-N-Edit Core per standard protocols. mRNA libraries were prepared with Universal Plus mRNA-Seq kit (NuGen) using 1000 ng input RNA. The size selection for libraries was performed using SPRIselect beads (Beckman Coulter) and purity of the libraries was analyzed using the High Sensitivity DNA chip on Bioanalyzer 2100 (Agilent). The prepared libraries were pooled and sequenced using NextSeq 500 (Illumina); generating ~20 million 2×76 bp paired-end reads per samples.

### RNA-Sequencing Transcriptome Analysis

The RNA-seq raw fastq data were processed with RNA-Seq Alignment app within the Illumina BaseSpace app suite ([www.basespace.illumina.com](http://www.basespace.illumina.com)): the adaptors were trimmed and reads were mapped to hg19 human reference genome using the STAR aligner (20) to generate BAM files, and FPKM estimation of reference genes and transcripts were performed using Cufflinks 2 (21). Based on this gene count matrix, we used “DESeq2” package (22) to identify differentially expressed genes between SHT5 cells versus CPCs. The significance level of FDR adjusted *p*-value of 0.05 was used to identify differentially expressed genes.

### Single-cell RNA-Sequencing Library Preparation and Sequencing

Cells were re-suspended in PBS with 0.04% BSA (Ambion) to a final concentration of 200 cells per µl on the day of single-cell capture and library preparation. This cell suspension was used as input for automated microfluidic single-cell capture and barcoding using the 10X Genomics Full Chromium platform. Approximately 560 single-cells were captured for each sample using the 10X Genomics Single Cell 3' Chip (as per manufacturer recommendations *Single Cell3' Re* version CG00052) at the University of Houston Seq-N-Edit Core. Single-cell gel beads in emulsion (GEMs) were generated and single cells were uniquely barcoded. cDNA was recovered and selected for using DynaBead MyOne Silane Beads (Thermo Fisher Scientific) and SPRIselect beads (Beckman Coulter). The library was indexed by addition of a 4 random 8 bp indexes “GCATCTCC” “TGTAAGGT” “CTGCGATG” and “CTGCGATG” which are Illumina sequencer compatible i7 indexes.

This sequence library then underwent quality control assessment by using a High-sensitivity DNA chip on 2100 BioAnalyzer (Agilent) and then quantified with a Qubit Fluorometer (Thermo Fisher Scientific) and with a Kapa Library Quantification Kit (Kapa Biosystems) by using the AriaMX instrument (Agilent). Libraries were sequenced using NextSeq 500 (Illumina) in stand-alone mode to obtain pair-end sequencing 26 bp (read1) X 98bp (read2) and a single index 8 bp in length obtaining ~40,000 reads per cell.

### Single-cell RNA-Sequencing Transcriptome Analysis

The single-cell RNA sequencing data analysis was performed on the Maxwell High-Performance Cluster at the University of Houston. The analytical program used was the Cell Ranger 2.1.1 Single Cell Analysis Pipelines (10X Genomics). Raw base call files generated by Nextseq 500 were demultiplexed using “cellranger mkfastq” pipeline to FASTQ files. FASTQ files were aligned to hg38 human reference genome using “cellranger count” which used STAR aligner (20). Gene expression matrix was reduced using Principal Components Analysis (PCA) and visualized in 2-d space by passing PCA data into t-distributed stochastic neighbor embedding (t-SNE), a nonlinear dimensionality reduction method (23). Graph-based hierarchical clustering algorithm operating in PCA space was used to cluster cells based on the similarity of expression. Differentially expressed genes between clusters were found using sSeq method (24). The top 100 differentially expressed genes from cluster-1 were used for gene ontology. The gene list was analyzed using Gene MANIA package on Cytoscape.

| Gene Ontology            | Gene List  | Q-value  |
|--------------------------|--|----------|
| Notch Signaling Pathway  | <i>Notch4, DLL4, Maml2, Maml3, PSENEN, APH1A, APH1B, NCSTN</i> | 9.50E-07 |
| Wnt Signaling Pathway    | <i>Wnt7B, FZD2, FZD10, FZD1, FZD4</i>                          | 5.30E-02 |
| Blood Vessel Development | <i>Wnt7b, FZD4, Notch4, DLL4, RPBJ</i>                         | 3.20E-02 |

Gene ontology of the top 100 differentially expressed genes from cluster-1.

### Statistics

Data were processed using GraphPad Prism 5.0 software and Microsoft Excel. The qPCR data and patch-clamp data are presented as the mean  $\pm$  standard deviation (S.D.) and mean  $\pm$  standard error of the mean (S.E.M.), respectively. For qPCR, the data were analyzed based on at least two independent experiments in three independent PCR reactions. Analysis of qPCR was performed using one-way ANOVA. Dunnett’s multiple comparison tests were performed on qPCR data for comparison of multiple groups with significant differences. Student’s *t*-test was used for statistical analysis to compare the control and positive groups for patch-clamp recording. A test was considered significant for  $p < 0.05$  and  $p < 0.001$ .

## RESULTS

### Conversion of CPCs into Pacemaker-like Cells Expressing CX30.2

The schematic diagram in Figure-1A shows the screening strategy for converting human CPCs into pacemaker cells (detailed in Figure-S1). Previously we reprogrammed human



adipogenic mesenchymal stem cells (hADMSCs) into cardiac progenitor cells (CPCs) that expressed the cardiac mesoderm marker  $KDR^+$  and cardiac-specific transfactor,  $NKX2.5$ , by using  $ETS2/MESP1$  human transcription factors. We have also shown that  $ETS2/MESP1$  effectively reprogrammed foreskin fibroblasts into CPCs (14). Here, we tested human transcription factors  $SHOX2$ ,  $TBX3$  channel protein  $HCN2$ , as reprogramming factors, to convert CPCs into Pacemaker-like cells. We used tetracycline-controlled transcriptional activation (tet-on) inducible reprogramming factors to regulate their transient expression within the CPCs. First, CPCs were transduced with the connexin 30.2 ( $CX30.2$ ) mCherry reporter, a conduction cell marker, followed by lentiviral vectors that provided doxycycline-induction of the reporter eGFP gene fused to either  $SHOX2$  (S),  $HCN2$  (H),  $TBX3$  (T3),  $TBX5$  (T5), and  $TBX18$  (T18) factors individually and in combinations (SHT3, SHT5, and SHT18). The  $CX30.2$  reporter gene is a slow conduction junction channel known to render the uncoupling characteristic of pacemaker tissue to the SAN (25) as well as being responsible for integrating all the pacemaker cells with different intrinsic frequency (26). The human orthologue of the mouse  $CX30.2$  gene is  $CX31.9$  and has been found in human ventricular biopsies of healthy individuals (27). Upon 3-days of doxycycline induction to transiently express the reprogramming factors, we observed eGFP<sup>+</sup> cells (Figure-1B; *left panel*) which were FACS sorted to obtain a pure population of eGFP<sup>+</sup> cells (Figure-1C, Figure-S2, and Figure-S3A–E). Transient expression of these reprogramming factors was validated by SDS/PAGE and antibodies for Western blot (Figure-S4).

A week later, we observed mCherry<sup>+</sup> cells (Figure-1B; right panel), the pacemaker-restricted cell marker, and FACS sorted the cells again to obtain a pure population of  $CX30.2$  reporter mCherry<sup>+</sup> cells (Figure-1C, Figure-S2, and Figure-S3F–J). All the reprogramming factors transduced singularly and in combinations generated a small population of cells positive for mCherry (Figure-1B; right panel and Figure-S3F–J). After cell sorting, we analyzed the percentage of mCherry<sup>+</sup> cells obtained from individual combinations of transcription factors to determine the percent conversion of CPCs to Pacemaker-like cells (Table-1). Our studies showed that SHT18 and SHT5 combination of transcription factors induced the highest percent conversion of 8.4% and 5.9% CPCs to become positive for  $CX30.2$ -mCherry expression. On the contrary, the channel factor  $HCN2$  (< 1%) had the lowest conversion rate for mCherry<sup>+</sup> cells.

### ***SHOX2*, *HCN2*, and *TBX5* (SHT5) Combination Drive Pacemaker Gene Expression**

A week after tet-on induced genes were silenced, we evaluated mCherry<sup>+</sup> cells for readout of pacemaker-specific target genes ( $CX30.2$ ,  $KCNN4$ ,  $HCN4$ ,  $HCN3$ ,  $HCN1$ , and  $SCN3b$  shown in Figure-2). Trio-factor combinations, such as SHT5 and SHT18 resulted in significant accumulation of  $CX30.2$  and  $KCNN4$  gene transcripts ( $p < 0.001$ ), in comparison to untreated control CPCs (Figure-2A&B).  $KCNN4$ , a calcium-activated potassium channel, is critical for functional Pacemaker-like activity (28, 29). Unlike  $Tbx5$  expression in murine ES cells which resulted in increased  $Cx30.2$  expression, here  $TBX5$  by itself did not increase  $CX30.2$  expression but required the combinatorial co-expression with  $SHOX2$  and  $HCN2$  to elevate  $CX30.2$  expression. (12). We observed the other individual reprogramming factors were also insufficient to raise the co-expression of  $CX30.2$  and  $KCNN4$ .  $HCN4$ , a potassium/sodium hyperpolarization-activated cyclic nucleotide-gated channel, is a

molecular marker for functional SAN cells activity, which initiates the funny current ( $I_f$ ), playing a crucial role in the pacemaker potential (9, 30, 31). Pacemaker ion channels *HCN1*, *HCN3*, and *HCN4* transcripts appeared in many of the mCherry+ cells, by the transient treatment of SHT5 (Figure-2C–E). Previously, *TBX3* was shown to upregulate the *HCN1* channels (32), which we confirmed (Figure-2E). Additionally, the *HCN2* channel factor influenced *HCN1* channel expression (Figure-2E). We also identified significant upregulation of *SCN3b* by the combination of SHT5 (Figure-2F). Interestingly, the knockout of *Scn3b* resulted in SAN abnormality in mice (33). Overall, the combination of *SHOX2*, *HCN2*, and *TBX5* (SHT5) transcription factors resulted in optimization of pacemaker-specific gene activity.

### Transient *SHOX2*, *HCN2*, and *TBX5* (SHT5) expression induced a Pacemaker Transcriptome Profile

To determine the transcriptome profiling of the reprogrammed cells, we performed RNA sequencing of SHT5 cells and CPCs. The principal component analysis (PCA) plot revealed that both the SHT5 and CPC samples within the plot grouped, as defined clusters and that the biological samples of each of these two cell types were clustered tightly (Figure-S5). The global heat map revealed that thousands of genes were differentially expressed between the SHT5 mCherry+ cells and the CPCs (Figure-3A). Furthermore, we identified that the SHT5 reprogrammed cells were enriched in pacemaker-specific markers including *SHOX2*, *GJD3* (*CX30.2*), *TBX5*, *TBX3*, *BMP2*, and *KCNN4* (Figure-3B), as reported by others (6, 34). In addition, the SHT5 cells also exhibited enrichment of pacemaker-specific transcripts for calcium and potassium channels including *KCND2*, *KCNK2*, *CACNB1*, and *CACNA1A* (32) (Figure-3B).

Previous studies showed that *NKX2.5* is not expressed in human and mouse SANs (35); whereas, *NKX2.5* is a specific ventricular conduction marker and highly enriched in Purkinje fibers (36). In addition to *NKX2.5*, *CNTN2* is also a specific ventricular conduction marker that is highly enriched in Purkinje fibers (36). In agreement with these studies, our data showed that Purkinje-restricted *NKX2.5* and *CNTN2* gene transcripts along with the cardiomyocyte-specific *GATA4* mRNA were not detectable in the SHT5 cells (Figure-3B). Similarly, Purkinje-specific *SCN5a* and *IRX6* gene transcript expression were not enriched in the SHT5 cells (Figure-3B) (36). However, our data did reveal expression of *IRX1*, *IRX2*, and *CNTN3*, markers of Purkinje cells, in SHT5 cells (Figure-3B) (36, 37).

These findings, therefore, raised a question of whether we have heterogeneity in the SHT5 population; hence, we decided to perform single-cell RNA sequencing on the SHT5 activated cells to better understand the transcriptome of the individual cells within the total cell population. In such, we captured 560 SHT5 cells and assessed the individual transcriptomes of each cell. We found four transcriptionally distinct clusters by graph-based hierarchical clustering, as represented in the t-distributed stochastic neighbor embedding (t-SNE) plot (Figure-3C). We observed that the cells in cluster-1 were enriched in the pacemaker-specific genes including *HCN2*, *HCN3*, *HCN4*, *SHOX2*, *GJC3*, and *BMP2* and thus consistent with the pacemaker phenotype (Figure-3D). We also found that while both cluster-3 and cluster-4 exhibited enrichment of few pacemaker genes, they also exhibited

low levels of *SHOX2* and *HCN2* (Figure-3D). Interestingly, we observed that clusters-1, cluster-3, and cluster-4 exhibited similarity in their downregulation of *NKX2.5*, *GATA4*, and *IRX3*. Thus, while *NKX2.5* downregulation drives the progenitor cells towards the pacemaker phenotype, its upregulation is essential for the Purkinje fiber upregulation (38–40). Consistent with our RNA sequencing data, we also did not observe an enrichment of *CNTN2*, a specific molecular marker for the Purkinje fibers, in the four clusters (Figure-3D). In contrast, cluster-2 exhibited upregulation of *HCN2* and *IRX3* as well as downregulation of *SHOX2*, *HCN3*, *HCN4*, among other genes thus possibly representing the heterogeneity of a non-pacemaker cell. Therefore, both RNA sequencing data and single-cell RNA sequencing data suggests that while having a population of cells which have all the three factors *SHOX2*, *HCN2*, and *TBX5* (*SHT5*) exhibiting the pacemaker phenotype, some cells were not converted into pacemaker cells. Non-converted cells may have occurred due to not receiving either one or two of the combination of transcription factors during lentiviral infection.

### ***SHOX2*, *HCN2*, and *TBX5* (*SHT5*) Combination Impose Functional Pacemaker Properties**

Based on the pacemaker gene expression profile with different transcription factors, we chose *SHT5* mCherry+ cells (Figure-4A) for the functional analysis. We observed that *SHT5* mCherry+ cells exhibited the *HCN4* current, and this *I<sub>h</sub>* current was absent in the control CPCs (Figure-4B). Specifically, cells were recorded with and without cesium (Cs<sup>+</sup>), where the Cs<sup>+</sup> sensitive fraction of the hyperpolarization-activated current was defined as the pacemaker current (i.e. funny current or the *HCN* current). The *SHT5* cells exhibited a robust *HCN4* inward current, characteristic of pacemaker cells. As expected, the addition of Cs<sup>+</sup> resulted in a complete blockade of *HCN* currents in the *SHT5* cells. We observed a significantly higher current density (pA/pF) of approximately 3-fold in *SHT5* cells ( $-5.03 \pm 1.36$  pA/pF, n=17) when compared to the CPCs ( $-1.12 \pm 0.64$  pA/pF, n=21) (Figure-4C). To further analyze the *HCN* channel activation kinetics, *SHT5* cells were given a series of hyperpolarization command followed by a depolarization step (Figure-4D), and the voltage that elicited 50% of the maximal response ( $V_{1/2}$ ) when *SHT5* cells were hyperpolarized from  $-55$  mV to  $-135$  mV was  $-125.28 \pm 3.83$  mV (n=14) (Figure-4E).

Biological pacemaker cells have the advantage of hormone regulation. The  $\beta$ -adrenergic receptor  $\beta$ -AR stimulated cAMP binds to the *HCN* channel and thereby contributes to the *HCN* pacemaker currents (41). To characterize the effect of  $\beta$ -AR stimulation on *HCNs*, we treated the *SHT5* cells with isoproterenol (ISO). The current density in *SHT5* cells increased significantly upon stimulation with ISO ( $-6.06 \pm 0.17$  pA/pF, n=9), as compared to the cells without ISO ( $-4.84 \pm 0.30$  pA/pF, n=8) (Figure-5A). Furthermore, treatment with ISO resulted in a significant shift of the *HCN* activation curve towards more positive voltages in the *SHT5* cells (Figure-5B) and the  $V_{1/2}$  was shifted from  $-125.6 \pm 4.66$  (n=8) in *SHT5* cells without ISO to  $-113.2 \pm 1.66$  (n=9) with ISO stimulation (Figure-5C). This result indicated that the *SHT5* cells exhibit functional *HCN* Pacemaker currents that are sensitive to  $\beta$ -AR stimulation.

## DISCUSSION

Over the last decade, a variety of transcription factors have been used to generate Pacemaker-like cells. In a recent study, Sun, Qiao (42) differentiated adipose-derived stem cells into Pacemaker-like cells through *TBX18*, while another study reported the conversion of the myocardial cells into the Pacemaker-like cell phenotype by ectopic expression of *TBX3* (32). In addition, *TBX5* overexpression in the *Xenopus laevis* model was shown to upregulate conduction system markers (12). During embryonic development of the heart, transcription factors *SHOX2*, *TBX3*, and *TBX5* regulated the SAN gene program (43). While other core factors, such as *TBX18* within the SAN have been shown to suppress cardiomyocyte formation (43). In another study, human mesenchymal stem cell (hMSCs) transduced with the mouse *Hcn2* gene generated funny currents, which was suggestive of the role of *Hcn2* in yielding functional biological pacemakers (44). Thus, to enhance our chance of reprogramming human CPCs into pacemaker cells, we decided to use the five factors singularly as well as in combination for reprogramming and the CX30.2 mCherry reporter, as a conversion endpoint.

Interestingly, our FACS sorting data yielded mCherry+ cells with all eight different combinations; by either employing *SHOX2*, *HCN2*, *TBX3*, *TBX5*, and *TBX18* transcription factors in single or SHT3, SHT5, and SHT18 transcription factors in combination. These results are consistent with previous studies where these transcription factors individually have resulted in driving the fate of substrate cells, both *in vitro* and *in vivo*, into Pacemaker-like cells. However converted mCherry+ cells from the SHT5 cocktail of transcription factors demonstrated the penultimate expression of many pacemaker specific genes; including, *CX30.2*, *KCNN4*, *HCN4*, *HCN3*, *HCN1*, and *SCN3b*. These findings suggest that the SHT5 combination of transcription factors is a much better candidate in driving the CPCs into Pacemaker-like cells than other combinations and single transcription factors. Further, we observed that the transcriptome of SHT5 cells exhibited enrichment of pacemaker specific genes including *TBX3*, *KCNN4*, *CX30.2*, and *BMP2*, as well as pacemaker specific calcium and potassium channels (*KCND2*, *KCNK2*, and *CACNB1*). In support of our findings, the transcriptome profile of our Pacemaker-like cells closely resembled the differentially expressed genes identified within the developing mouse SAN (45). In addition, similar to human and mouse SAN studies, we observed the down-regulation of *NKX2.5*. Thus, the transcriptome data and gene assay data revealed that the SHT5 activated cells that share a pacemaker cell phenotype.

To determine the functional efficiency of the reprogrammed cells using the SHT5 combination of transcription factors, we measured the *HCN* current using patch-clamp recordings, which is characteristic in pacemaker cells. We recorded the hyperpolarization-elicited inward currents with the current density at  $-5.03 \pm 1.36$  pA/pF when the SHT5 cells were hyperpolarized from  $-40$  to  $-130$  mV ( $n=17$ ). Further, the voltage to elicit half of the maximal *HCN* current ( $V_{1/2}$ ) was around  $-125$  mV when SHT5 cells were recorded with a series of hyperpolarization steps (from  $-55$  mV to  $-135$  mV; the maximal current was elicited at  $-135$  mV). In a recent study, Kapoor, Liang (46) transduced *Tbx18* in ventricular myocytes of rats to generate biological pacemaker. They reported that the transduced cells recorded  $I_f$  with a current density of  $-1.9 \pm 0.8$  pA/pF at  $-50$  mV ( $n=3$ ). In another study,

Yang, Zhang (13) induced differentiation of ADSC using *Tbx18* to generate Pacemaker-like cells. They reported that the differentiated Pacemaker-like cells exhibited a current density of  $-5.43 \pm 1.36$  pA/pF (n=4). In addition, previous studies have shown that cyclic AMP (cAMP) modulates cardiac pacemaker *HCN* currents and shifts the activation curve to more positive voltages (47). Our studies also showed that the *HCN* currents recorded in the SHT5 mCherry+ cells were sensitive to  $\beta$ -AR stimulation by ISO, increasing the current density and shifting the  $V_{1/2}$  to a more positive voltage ( $-113$  mV). Thus, our SHT5 converted Pacemaker-like cells exhibited *HCN* currents demonstrated functional characteristics of pacemaker cells.

## CONCLUSIONS

In our study, we observed that the *SHOX2*, *HCN2*, and *TBX5* (SHT5) cocktail of transcription factors and channel protein reprogrammed the CPCs into Pacemaker-like cells. The SHT5 factors resulted in upregulation of pacemaker specific gene expression and transcriptome expression, attributing the pacemaker phenotype to these cells. In addition, the SHT5 cells also exhibited the functional characteristic of pacemaker cells (i.e.  $I_f$  recording). Thus, the SHT5 combination of transcription factors and channel protein are able to reprogram human CPCs into human cardiac Pacemaker-like cells and will facilitate the development of cell-based therapies for various cardiac conduction diseases.

## Supplementary Material

Refer to Web version on PubMed Central for supplementary material.

## ACKNOWLEDGMENTS

The data in this paper are based on the dissertation thesis submitted in partial fulfillment of the requirements for a Ph.D. (Pharmacology) in the Department of Pharmacological and Pharmaceutical Sciences in the College of Pharmacy at the University of Houston (S.R.).

### FUNDING:

Research reported in this paper was supported in part by the National Heart, Lung, and Blood Institute (NHLBI) of the National Institutes of Health (NIH) [R15HL141963 (B.K.M.) and R15HL124458 (B.K.M.)], the American Heart Association (AHA) [18AIREA33960175 (to B.K.M.)], and a grant from Robert J. Kleberg, Jr. and Helen C. Kleberg Foundation (to B.K.M.). The Center for Advanced Science in Space supported research on the conversion of human adipogenic mesenchymal stem cells into cardiac progenitors (R.J.S.). The funders had no role in study design, data collection, and analysis, decision to publish, or preparation of the manuscript.

## ABBREVIATIONS

|                              |                              |
|------------------------------|------------------------------|
| <b>AVN</b>                   | atrioventricular node        |
| <b>cAMP</b>                  | cyclic AMP                   |
| <b><math>\beta</math>-AR</b> | $\beta$ -adrenergic receptor |
| <b>CCS</b>                   | cardiac conduction system    |
| <b>CNTN</b>                  | contactin                    |

|                       |  |
|-----------------------|--|
| <b>CPCs</b>           | cardiac progenitor cells   |
| <b>Cs<sup>+</sup></b> | cesium   |
| <b>CsCl</b>           | cesium chloride  |
| <b>CVD</b>            | cardiovascular disease   |
| <b>Cx</b>             | connexins  |
| <b>ESC</b>            | embryonic stem cells   |
| <b>ETS</b>            | E26 transformation-specific  |
| <b>eGFP</b>           | enhanced green fluorescent protein   |
| <b>HCN</b>            | potassium/sodium hyperpolarization-activated cyclic nucleotide-gated channel |
| <b>HF</b>             | heart failure  |
| <b>hADMSCs</b>        | human adipogenic mesenchymal stem cells                                      |
| <b>hMSCs</b>          | human mesenchymal stem cells   |
| <b>I<sub>f</sub></b>  | funny current  |
| <b>IRX</b>            | iroquois   |
| <b>ISO</b>            | isoproterenol  |
| <b>KCNN4</b>          | potassium calcium-activated channel subfamily N member 4                     |
| <b>MSC</b>            | mesenchymal stem cells   |
| <b>MESP</b>           | mesoderm posterior protein   |
| <b>MI</b>             | myocardial infarction  |
| <b>NKX2.5</b>         | NK2 transcription factor related, locus 5                                    |
| <b>pA/pF</b>          | current density  |
| <b>PCA</b>            | principal component analysis   |
| <b>PCR</b>            | polymerase chain reaction  |
| <b>SAN</b>            | sinoatrial node  |
| <b>SCN</b>            | sodium channel   |
| <b>SCN3b</b>          | sodium voltage-gated channel beta subunit-3                                  |
| <b>SHOX2</b>          | short stature homeobox 2   |
| <b>SSS</b>            | sick sinus syndrome  |



|              |  |
|--------------|--|
| <b>t-SNE</b> | t-distributed stochastic neighbor embedding plot |
| <b>TBX3</b>  | T-box transcription factor 3                     |
| <b>TBX5</b>  | T-box transcription factor 5                     |
| <b>TBX18</b> | T-box transcription factor 18                    |

## References

1. Mangoni ME, Nargeot J. Genesis and regulation of the heart automaticity. *Physiol Rev.* 2008;88(3):919–82. [PubMed: 18626064]
2. John RM, Kumar S. Sinus Node and Atrial Arrhythmias. *Circulation.* 2016;133(19):1892–900. [PubMed: 27166347]
3. Alonso A, Jensen PN, Lopez FL, Chen LY, Psaty BM, Folsom AR, et al. Association of sick sinus syndrome with incident cardiovascular disease and mortality: the Atherosclerosis Risk in Communities study and Cardiovascular Health Study. *PLoS One.* 2014;9(10):e109662. [PubMed: 25285853]
4. Echt DS, Liebson PR, Mitchell LB, Peters RW, Obias-Manno D, Barker AH, et al. Mortality and morbidity in patients receiving encainide, flecainide, or placebo. The Cardiac Arrhythmia Suppression Trial. *N Engl J Med.* 1991;324(12):781–8. [PubMed: 1900101]
5. Boyett MR, Honjo H, Kodama I. The sinoatrial node, a heterogeneous pacemaker structure. *Cardiovasc Res.* 2000;47(4):658–87. [PubMed: 10974216]
6. Vedantham V New Approaches to Biological Pacemakers: Links to Sinoatrial Node Development. *Trends Mol Med.* 2015;21(12):749–61. [PubMed: 26611337]
7. Christoffels VM, Mommersteeg MT, Trowe MO, Prall OW, de Gier-de Vries C, Soufan AT, et al. Formation of the venous pole of the heart from an Nkx2–5-negative precursor population requires Tbx18. *Circ Res.* 2006;98(12):1555–63. [PubMed: 16709898]
8. Burkhard S, van Eif V, Garric L, Christoffels VM, Bakkens J. On the Evolution of the Cardiac Pacemaker. *J Cardiovasc Dev Dis.* 2017;4(2).
9. Espinoza-Lewis RA, Yu L, He F, Liu H, Tang R, Shi J, et al. Shox2 is essential for the differentiation of cardiac pacemaker cells by repressing Nkx2–5. *Dev Biol.* 2009;327(2):376–85. [PubMed: 19166829]
10. Mommersteeg MT, Hoogaars WM, Prall OW, de Gier-de Vries C, Wiese C, Clout DE, et al. Molecular pathway for the localized formation of the sinoatrial node. *Circ Res.* 2007;100(3):354–62. [PubMed: 17234970]
11. Singh R, Hoogaars WM, Barnett P, Grieskamp T, Rana MS, Buermans H, et al. Tbx2 and Tbx3 induce atrioventricular myocardial development and endocardial cushion formation. *Cell Mol Life Sci.* 2012;69(8):1377–89. [PubMed: 22130515]
12. Herrmann F, Bundschu K, Kuhl SJ, Kuhl M. Tbx5 overexpression favors a first heart field lineage in murine embryonic stem cells and in *Xenopus laevis* embryos. *Dev Dyn.* 2011;240(12):2634–45. [PubMed: 22072574]
13. Yang M, Zhang GG, Wang T, Wang X, Tang YH, Huang H, et al. TBX18 gene induces adipose-derived stem cells to differentiate into pacemaker-like cells in the myocardial microenvironment. *Int J Mol Med.* 2016;38(5):1403–10. [PubMed: 27632938]
14. Islas JF, Liu Y, Weng KC, Robertson MJ, Zhang S, Prejusa A, et al. Transcription factors ETS2 and MESP1 transdifferentiate human dermal fibroblasts into cardiac progenitors. *Proc Natl Acad Sci U S A.* 2012;109(32):13016–21. [PubMed: 22826236]
15. Gimble JM, Katz AJ, Bunnell BA. Adipose-derived stem cells for regenerative medicine. *Circ Res.* 2007;100(9):1249–60. [PubMed: 17495232]
16. Rangappa S, Entwistle JW, Wechsler AS, Kresh JY. Cardiomyocyte-mediated contact programs human mesenchymal stem cells to express cardiogenic phenotype. *J Thorac Cardiovasc Surg.* 2003;126(1):124–32. [PubMed: 12878947]

17. Yamada Y, Wang XD, Yokoyama S, Fukuda N, Takakura N. Cardiac progenitor cells in brown adipose tissue repaired damaged myocardium. *Biochem Biophys Res Commun.* 2006;342(2):662–70. [PubMed: 16488397]
18. Spandidos A, Wang X, Wang H, Seed B. PrimerBank: a resource of human and mouse PCR primer pairs for gene expression detection and quantification. *Nucleic Acids Res.* 2010;38(Database issue):D792–9. [PubMed: 19906719]
19. Shi L, Chang JY, Yu F, Ko ML, Ko GY. The Contribution of L-Type Cav1.3 Channels to Retinal Light Responses. *Front Mol Neurosci.* 2017;10:394. [PubMed: 29259539]
20. Dobin A, Davis CA, Schlesinger F, Drenkow J, Zaleski C, Jha S, et al. STAR: ultrafast universal RNA-seq aligner. *Bioinformatics.* 2013;29(1):15–21. [PubMed: 23104886]
21. Trapnell C, Hendrickson DG, Sauvageau M, Goff L, Rinn JL, Pachter L. Differential analysis of gene regulation at transcript resolution with RNA-seq. *Nat Biotechnol.* 2013;31(1):46–53. [PubMed: 23222703]
22. Love MI, Huber W, Anders S. Moderated estimation of fold change and dispersion for RNA-seq data with DESeq2. *Genome Biol.* 2014;15(12):550. [PubMed: 25516281]
23. Lvd Maaten. Accelerating t-SNE using Tree-Based Algorithms. *Journal of Machine Learning Research.* 2018;15:3221–45.
24. Yu D, Huber W, Vitek O. Shrinkage estimation of dispersion in Negative Binomial models for RNA-seq experiments with small sample size. *Bioinformatics (Oxford, England).* 292013 p. 1275–82.
25. Kreuzberg MM, Sohl G, Kim JS, Verselis VK, Willecke K, Bukauskas FF. Functional properties of mouse connexin30.2 expressed in the conduction system of the heart. *Circ Res.* 2005;96(11):1169–77. [PubMed: 15879306]
26. Verheijck EE, van Kempen MJ, Veereschild M, Lurvink J, Jongsma HJ, Bouman LN. Electrophysiological features of the mouse sinoatrial node in relation to connexin distribution. *Cardiovasc Res.* 2001;52(1):40–50. [PubMed: 11557232]
27. Munshi NV, McAnally J, Bezprozvannaya S, Berry JM, Richardson JA, Hill JA, et al. Cx30.2 enhancer analysis identifies Gata4 as a novel regulator of atrioventricular delay. *Development.* 2009;136(15):2665–74. [PubMed: 19592579]
28. Kleger A, Seufferlein T, Malan D, Tischendorf M, Storch A, Wolheim A, et al. Modulation of calcium-activated potassium channels induces cardiogenesis of pluripotent stem cells and enrichment of pacemaker-like cells. *Circulation.* 2010;122(18):1823–36. [PubMed: 20956206]
29. Kleger A, Liebau S. Calcium-activated potassium channels, cardiogenesis of pluripotent stem cells, and enrichment of pacemaker-like cells. *Trends Cardiovasc Med.* 2011;21(3):74–83. [PubMed: 22626246]
30. Christoffels VM, Smits GJ, Kispert A, Moorman AF. Development of the pacemaker tissues of the heart. *Circ Res.* 2010;106(2):240–54. [PubMed: 20133910]
31. Stieber J, Herrmann S, Feil S, Loster J, Feil R, Biel M, et al. The hyperpolarization-activated channel HCN4 is required for the generation of pacemaker action potentials in the embryonic heart. *Proc Natl Acad Sci U S A.* 2003;100(25):15235–40. [PubMed: 14657344]
32. Bakker ML, Boink GJ, Boukens BJ, Verkerk AO, van den Boogaard M, den Haan AD, et al. T-box transcription factor TBX3 reprogrammes mature cardiac myocytes into pacemaker-like cells. *Cardiovasc Res.* 2012;94(3):439–49. [PubMed: 22419669]
33. Hakim P, Brice N, Thresher R, Lawrence J, Zhang Y, Jackson AP, et al. Scn3b knockout mice exhibit abnormal sino-atrial and cardiac conduction properties. *Acta Physiol (Oxf).* 2010;198(1):47–59. [PubMed: 19796257]
34. Puskaric S, Schmitteckert S, Mori AD, Glaser A, Schneider KU, Bruneau BG, et al. Shox2 mediates Tbx5 activity by regulating Bmp4 in the pacemaker region of the developing heart. *Hum Mol Genet.* 2010;19(23):4625–33. [PubMed: 20858598]
35. Espinoza-Lewis RA, Liu H, Sun C, Chen C, Jiao K, Chen Y. Ectopic expression of Nkx2.5 suppresses the formation of the sinoatrial node in mice. *Dev Biol.* 2011;356(2):359–69. [PubMed: 21640717]

36. Maass K, Shekhar A, Lu J, Kang G, See F, Kim EE, et al. Isolation and characterization of embryonic stem cell-derived cardiac Purkinje cells. *Stem Cells*. 2015;33(4):1102–12. [PubMed: 25524238]
37. Pallante BA, Giovannone S, Fang-Yu L, Zhang J, Liu N, Kang G, et al. Contactin-2 expression in the cardiac Purkinje fiber network. *Circ Arrhythm Electrophysiol*. 2010;3(2):186–94. [PubMed: 20110552]
38. Harris BS, Spruill L, Edmonson AM, Rackley MS, Benson DW, O'Brien TX, et al. Differentiation of cardiac Purkinje fibers requires precise spatiotemporal regulation of Nkx2–5 expression. *Dev Dyn*. 2006;235(1):38–49. [PubMed: 16245335]
39. Jay PY, Harris BS, Maguire CT, Buerger A, Wakimoto H, Tanaka M, et al. Nkx2–5 mutation causes anatomic hypoplasia of the cardiac conduction system. *J Clin Invest*. 2004;113(8):1130–7. [PubMed: 15085192]
40. Schott JJ, Benson DW, Basson CT, Pease W, Silberbach GM, Moak JP, et al. Congenital heart disease caused by mutations in the transcription factor NKX2–5. *Science*. 1998;281(5373):108–11. [PubMed: 9651244]
41. Biel M, Michalakos S. Cyclic nucleotide-gated channels. *Handb Exp Pharmacol*. 2009(191):111–36.
42. Sun AJ, Qiao L, Huang C, Zhang X, Li YQ, Yang XQ. Comparison of mouse brown and white adiposederived stem cell differentiation into pacemakerlike cells induced by TBX18 transduction. *Mol Med Rep*. 2018;17(5):7055–64. [PubMed: 29568953]
43. van Weerd JH, Christoffels VM. The formation and function of the cardiac conduction system. *Development*. 2016;143(2):197–210. [PubMed: 26786210]
44. Bruzauskaite I, Bironaite D, Bagdonas E, Skeberdis VA, Denkovskij J, Tamulevicius T, et al. Relevance of HCN2-expressing human mesenchymal stem cells for the generation of biological pacemakers. *Stem Cell Res Ther*. 2016;7(1):67. [PubMed: 27137910]
45. Goodyer WR, Beyersdorf BM, Paik DT, Tian L, Li G, Buikema JW, et al. Transcriptomic Profiling of the Developing Cardiac Conduction System at Single-Cell Resolution. *Circ Res*. 2019;125(4):379–97. [PubMed: 31284824]
46. Kapoor N, Liang W, Marban E, Cho HC. Direct conversion of quiescent cardiomyocytes to pacemaker cells by expression of Tbx18. *Nat Biotechnol*. 2013;31(1):54–62. [PubMed: 23242162]
47. DiFrancesco D, Tortora P. Direct activation of cardiac pacemaker channels by intracellular cyclic AMP. *Nature*. 1991;351(6322):145–7. [PubMed: 1709448]

**HIGHLIGHTS**

*SHOX2, HCN2, and TBX5* (SHT5) cocktail of transcription factors and channel protein reprogrammed CPCs into Pacemaker-like cells. The SHT5 factors resulted in upregulation of pacemaker specific gene expression and transcriptome expression, attributing the pacemaker phenotype to the cells. The SHT5 mCherry+ cells also exhibited the funny current via *HCN4* channels, attributing the functional characteristic of pacemaker cells. Thus, the findings of this study show that the SHT5 combination of transcription factors can be used to reprogram CPCs into Pacemaker-like cells as a potential stem cell therapy for sick sinus syndrome (SSS) as well as for other cardiac conduction diseases.

Author Manuscript

Author Manuscript

Author Manuscript

Author Manuscript

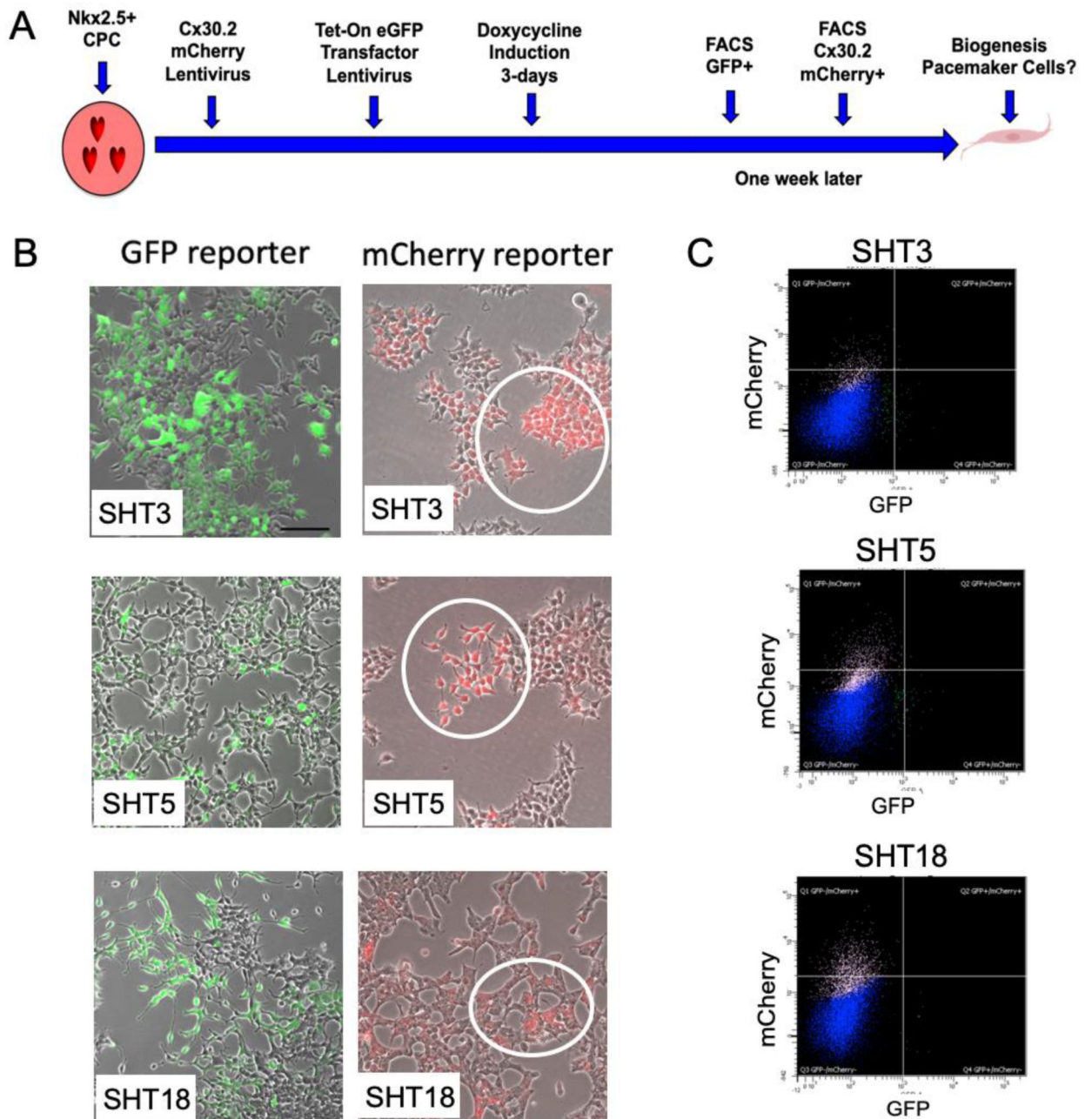


**Figure-1: Conversion of human CPCs into Pacemaker-like cells.**

(A) Schematic showing a screening strategy by which reprogrammed CPCs are engineered into Pacemaker-like cells. Initially, all the CPCs were infected with CX30.2 mCherry reporter lentivirus, followed by infection with tet-on inducible transcription factors singularly and/or in combination. Transient 3-day induction of doxycycline was carried out to induce the expression of transcription factors, followed by FACS sorting for eGFP<sup>+</sup> cells. A week later, when mCherry<sup>+</sup> cells were observed under the microscope, reprogrammed cells were FACS sorted for a pure population of mCherry<sup>+</sup> cells. These mCherry<sup>+</sup> cells were further analyzed by RT-qPCR, RNA sequencing and single-cell RNA sequencing for expression analysis and whole-cell patch-clamp analysis for functional efficiency (i.e.

biogenesis of cardiac Pacemaker-like cells). **(B)** Fluorescence microscopy of the reprogrammed CPCs for GFP+ cells and mCherry+ cells after FACS sorting. Reprogramming was induced by the addition of 1 µg/ml doxycycline to tet-on lentivirus-transduced CPCs for 3-days with the transcription factors, both individually and in combination. *Images on the left* show eGFP+ cells that were treated with a combination of transcription factors (SHT3, SHT5, and SHT18). Following an additional 7-days, CPCs that were initially transduced with the CX30.2 mCherry reporter genespecific for cardiac pacemaker cells were observed for mCherry+ expression. *Images on the right* show mCherry + cells treated with the combination of transcription factors (SHT3, SHT5, and SHT18). SHT5 and SHT18 generated the highest conversion rate of cell positive for mCherry labeled CX30.2 (5.9% and 8.43%, respectively). Note the mCherry+ labeling of the reprogrammed CPCs (*circled*). **(C)** FACS plots showing sorting of the transduced CPCs for mCherry+ cells (CX30.2) following induction of the transcription factors in combinations (SHT3, SHT5, and SHT18).



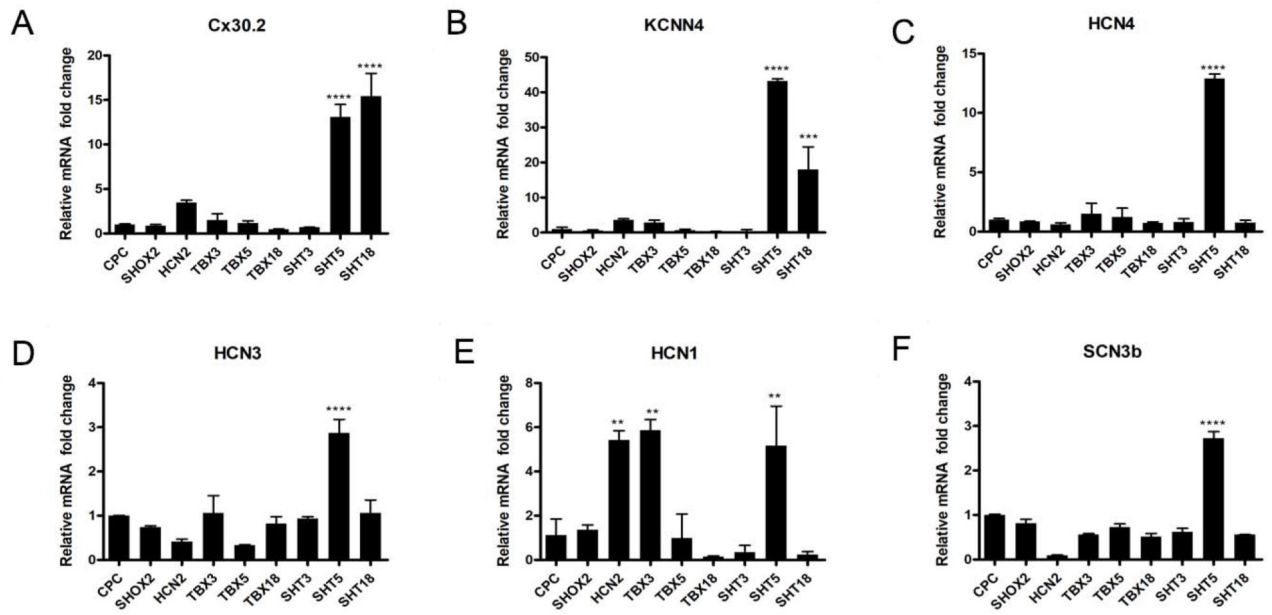


**Figure-2: Expression of Pacemaker Specific Genes.**

RT-PCR of the reprogrammed CPCs for expression of pacemaker specific genes: (A) CX30.2, (B) KCNN4, (C) *HCN4*, (D) *HCN3*, (E) *HCN1*, and (F) *SCN3b*. CX30.2 and KCNN4 were significantly expressed in cells treated with the SHT5 and SHT18 combination of transcription factors. Similarly, expression of the *HCN4* and *HCN3* ion channels were significantly increased in cells treated with the SHT5 combination. However, while *HCN1* expression was significantly increased in cells active by *HCN2*, *TBX3*, and SHT5 transcription factors, *SCN3b* expression was only increased in SHT5 activated cells. One-way ANOVA followed by Dunnett's multiple comparison tests was applied for RT-PCR analysis. All data are expressed as mean  $\pm$  SD. A significance level of \*\* $p < 0.05$ , \*\*\* $p < 0.001$ , \*\*\*\* $p < 0.0001$  versus CPCs is indicated by an asterisk(s).

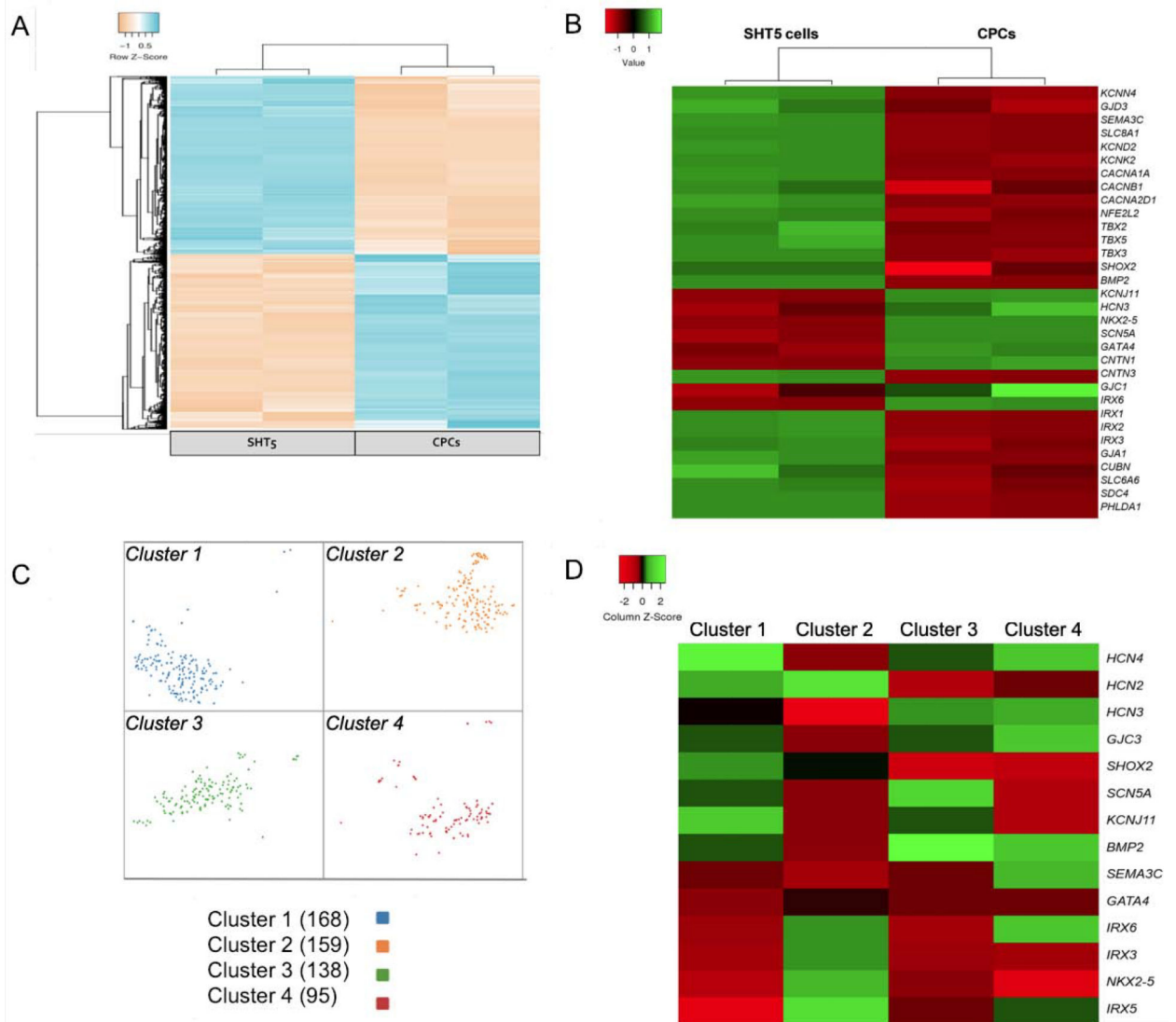


**Figure-3: Transcriptome analysis of SHT5 reprogrammed cells.**

Transcriptome analysis of SHT5 reprogrammed human CPCs into Pacemaker-like cells were characterized by both RNA sequencing and single-cell RNA sequencing. **(A)** Heat map displaying thousands of genes that are differentially expressed (adjusted  $p$ -value < 0.05) between SHT5 and CPCs indicating a change in transcriptome during reprogramming. **(B)** Heat map of SHT5 cells and CPCs showing differentially expressed (adjusted  $p$ -value < 0.05) transcriptome of genes marking the pacemaker phenotype. **(C)** A t-distributed stochastic neighbor embedding (t-SNE) plot from the single-cell RNA sequencing of 560 SHT5 cells showing the distribution in four distinctive clusters. **(D)** Heat map displaying differentially expressed genes between four clusters of SHT5 cells (adjusted  $p$ -value < 0.05); cluster 1 (blue), cluster 2 (orange), cluster 3 (green), and cluster 4 (red).

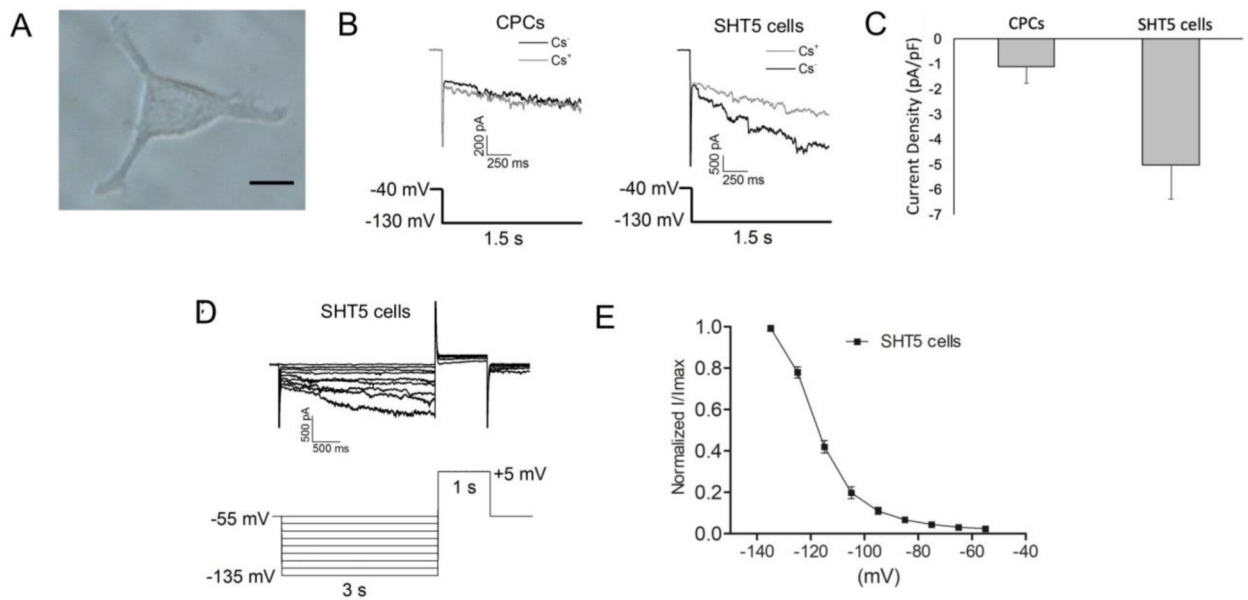


**Figure-4: Whole Cell electrophysiological recordings of functional SHT5 reprogrammed cells.** (A) A representative image of an SHT5 mCherry+ cell used for the electrophysiological recording. (B) Whole-cell current traces were recorded from the CPCs (*left panel*) or the SHT5 mCherry+ (*HCN* positive) cells (*right panel*) in the absence (gray) and presence (black) of 5 mM Cs<sup>+</sup>. The voltage protocol is indicated below the traces. The *HCN* current was defined as the Cs<sup>+</sup>-sensitive fraction of the hyperpolarization-activated current. (C) The current density (pA/pF) from SHT5 cells ( $-5.03 \pm 1.36$ ,  $n=17$ ) is significantly higher than the current density recorded from CPCs ( $-1.12 \pm 0.64$ ,  $n=21$ ). (D) A series hyperpolarizing step command followed by a depolarization step was applied to determine the channel activation kinetics. Traces recorded from a representative SHT5 cell is shown. (E) The Cs<sup>+</sup> sensitive current at each voltage-step (*I*) was normalized to the peak current (*I*<sub>max</sub> at  $-135$  mV), and the *I*/*I*<sub>max</sub> was plotted then fitted with the Boltzmann equation:  $I/I_{max} = 1 / [1 + \exp((V_{1/2} - V) / k)]$ . The voltage eliciting half of the maximal current (*I*/*I*<sub>max</sub> at 0.5) was calculated as  $-125.28 \pm 3.83$  mV for the SHT5 (*HCN4* positive) cells ( $n=14$ ).

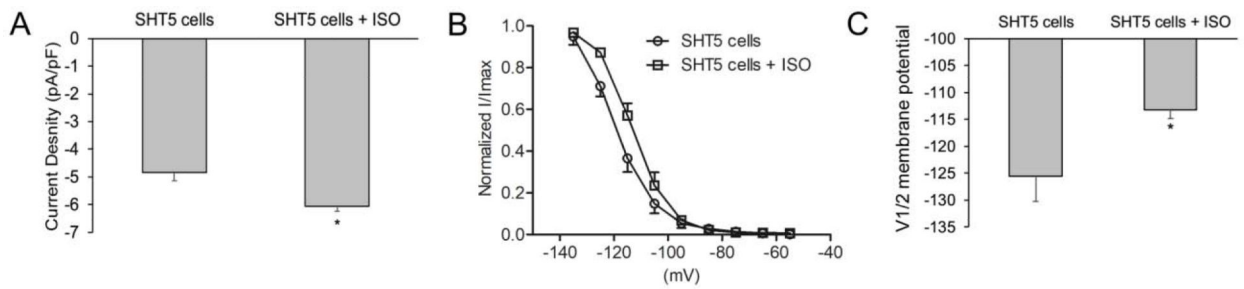


**Figure-5: Electrophysiological recordings in the presence of beta-adrenergic receptor stimulation with Isoproterenol (ISO).**

(A) Treatment with 100 nM isoproterenol (ISO) significantly increased the *HCN4* current density (pA/pF) in SHT5 mCherry+ cells (SHT5:  $-4.84 \pm 0.30$  pA/pF, n=8; SHT5+ISO:  $-6.06 \pm 0.17$  pA/pF, n=9) (B) Treatment with ISO also shifted the activation curve toward more positive voltages in SHT5 mCherry+ cells. (C) ISO shifted the activation midpoint  $V_{1/2}$  significantly to a more positive voltage in SHT5 mCherry+ cells (SHT5:  $V_{1/2} = -125.6 \pm 4.66$  mV, n=8; SHT5+ISO:  $-113.2 \pm 1.66$ , n=9). All data are presented as a mean  $\pm$  SEM. The Student's *t*-test was used for statistical analysis, \*  $p < 0.05$ .

**Table-1:**  
**Quantification of mCherry+ cells from FACS analyses to determine the percentage of conversion.**

SHT5 and SHT18 cells exhibited a higher conversion rate, while *HCN2* showed the lowest conversion rate.

| Transcription Factor Combinations | % mCherry+ Cells |
|-----------------------------------|------------------|
| SHOX2                             | 2.40             |
| HCN2                              | 0.22             |
| TBX3                              | 4.11             |
| TBX5                              | 2.64             |
| TBX18                             | 5.45             |
| SHOX2-HCN2-TBX3 (SHT3)            | 1.74             |
| SHOX2-HCN2-TBX5 (SHT5)            | 5.90             |
| SHOX2-HCN2-TBX18 (SHT18)          | 8.43             |

Author Manuscript

Author Manuscript

Author Manuscript

Author Manuscript